Small-Signal Model of a 5kW High-Output Voltage Capacitive-Loaded Series-Parallel Resonant DC-DC Converter

Fabiana da Silveira Cavalcante and Johann W. Kolar
Swiss Federal Institute of Technology (ETH) Zurich
Power Electronic Systems Laboratory
ETH Zentrum / ETL I14, Physikstrasse 3
CH-8092 Zurich / SWITZERLAND
cavalcante@lem.ee.ethz.ch kolar@lem.ee.ethz.ch

Abstract — This paper presents an accurate method, based on first harmonic analysis, to derive the small-signal model of the series-parallel resonant DC-DC converter with capacitive output filter for high-voltage applications. The model provides a fast and reliable way to obtain the desired transfer functions of the system for each operating point. For this reason, the small-signal model simplifies the controller design task for resonant converters by removing the need of complex mathematical analysis and saves the time required for measurements when using trial and error design method. The small-signal model has been verified through simulation and experimental measurements.

I. INTRODUCTION

Series-parallel resonant converters are frequently employed for the realization of high output voltage DC-DC converters since they can integrate the non-idealities of the high-voltage transformer. However, the design of resonant converters is involved due to the large number of operating states occurring within a pulse period [1]. Specifically, the controller design task is involved because the small-signal transfer function is extremely dependent on the operating point of the converter. There are a large number of representative publications on modeling and control of resonant converters where small-signal models for the series, parallel and inductive loaded series-parallel resonant converters are proposed [2,4,5,6]. However the small-signal model of the capacitive loaded series-parallel resonant converter is still missing from the literature and for this reason many controller designs are performed by trial and error [7]. The trial and error procedure is not convenient because the small-signal model varies significantly with load changes and the load is normally an unknown parameter. Therefore, the setting of the controller parameters can take a long time until a robust set of parameters are found.

This paper develops a small-signal model for the series-parallel resonant DC-DC converter with capacitive output filter in order to make the controller design for this type of converter easier. The converter power circuit is initially described and an analytical description of the transient and steady-state behavior is given based on the generalized averaging method [2]. Furthermore, the small-signal model of the converter is determined and the magnitude and phase plots of the transfer function of the control variable to the output voltage are shown. Results from simulations of a 5kW converter with output voltage in the range from 23kV to 62.5kV and operating at 250 kHz at full load and 500 kHz at low load, are given. The simulation results fully verify the theoretical considerations. Finally, the accuracy of the small-signal model is verified by a laboratory prototype.

II. CIRCUIT DESCRIPTION

The topology of the 5kW series-parallel resonant full-bridge DC-DC converter with impressed output voltage, operating above resonance, is shown in **Fig. 1**. The (parasitic) capacitors C_1, C_3 serve for zero-voltage switching of power transistors S_1 and S_3, the resonant inductor L_s is formed by the transformer stray inductance in combination with an auxiliary inductor connected in series. The parallel resonant capacitor C_p is formed by the parasitic capacitance of the high-voltage transformer T_1 secondary winding. The converter output power is controlled by varying the duty-cycle and the operating frequency is automatically adjusted to ensure the commutation of one bridge leg occurs at zero current. This bridge leg is realized with IGBTs and additional diodes, D_2, and D_4. The second bridge leg commutates at zero voltage, therefore power MOSFETs are employed and the free-wheeling diodes D_1, D_3 are the intrinsic diodes of the MOSFETs.

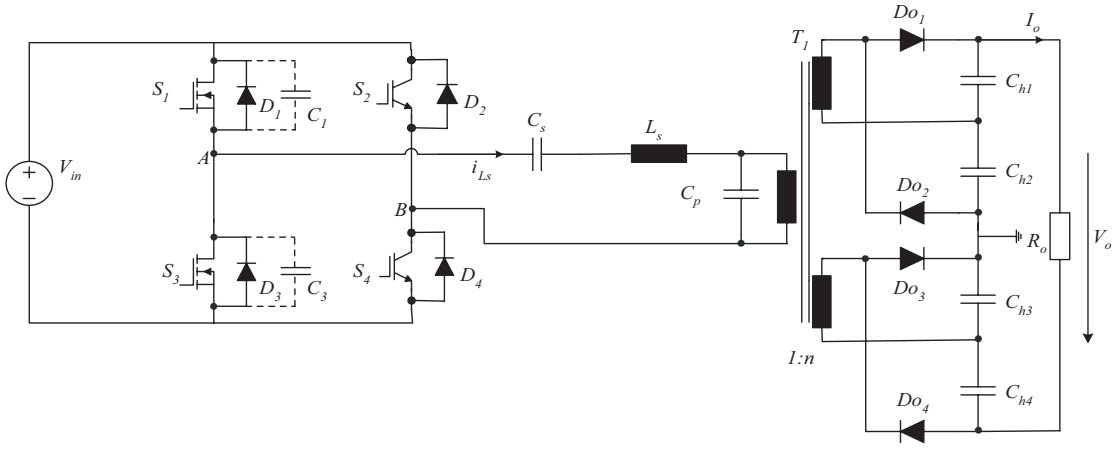

Fig. 1: Structure of the power circuit of a series-parallel resonant DC/DC converter with impressed output voltage; C_p denotes the equivalent capacitance of the secondary winding referred to the primary.

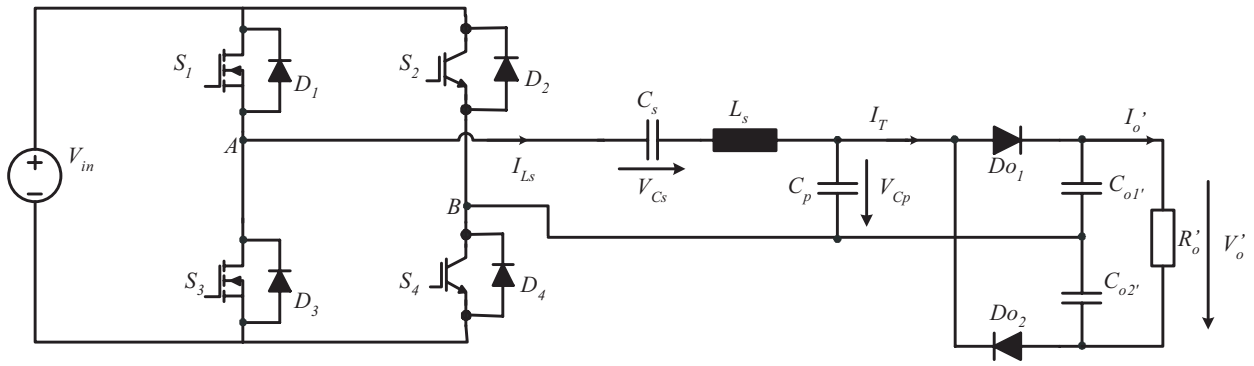

Fig. 2: Simplified circuit of the converter with the output components referred to the transformer primary side.

In order to simplify the analysis it is assumed that: all the components are ideal and have no losses; the voltage, V_{in}, supplied by the input pre-regulator is constant and has no ripple; the magnetizing inductance of the transformer is not considered in the analysis; capacitors C_1,C_3, are too small so they are not included in the analysis; the load is modeled as a pure resistance and all the output quantities are referred to the transformer primary side. From these assumptions the simplified model of the converter can be represented by the circuit of the **Fig. 2.**

The converter system is designed with following parameters, which is representative of the experimental system:

V_{in} = 325V	V_o = 23kV…62.5kV
I_o = 0…200mA	P_o = 0…5kW
n = 15	f_s = 250kHz….500kHz
C_s = 30nF	C_p = 12nF
L_s = 24.3µH	C_{o1}', C_{o2}' = 0.5µF

The equivalent output voltage, output current and output resistance, referred to the primary side of transformer, are respectively: $V_{o'} = V_o/2n$, $I_{o'} = I_o \cdot 2n$ and $R_{o'} = R_o/4n^2$ where n is the transformer turns ratio.

III. THEORETICAL ANALYSIS

A. Nonlinear Model of the Series-Parallel Resonant Converter

State space averaging has been demonstrated to be an effective method for analysis and control design in PWM switching power converters. However the method cannot be applied to a wide range of power circuits that includes the resonant type converters. The basic limitation in resonant converters is that these circuits have state variables with a predominantly oscillatory behavior. The generalized averaging method overcomes the limitations of the state-space averaging method because it can describe arbitrary types of waveforms [2]. The method is based on the fact that the waveform $x(\bullet)$ can be approximated in the interval $(t-T, t]$ with a Fourier series representation of the form

$$x(t-T+s) = \sum_k \langle x \rangle_k (t) e^{jk\omega_s (t-T+s)} \tag{1}$$

where the sum is over all integers k, $\omega_s = 2\pi/T$, $s \in (0, T]$, and $\langle x \rangle_k(t)$ are complex Fourier coefficients.

The time derivative of the k^{th} coefficient is computed to be

$$\frac{d}{dt}\langle x \rangle_k (t) = \left\langle \frac{d}{dt} x \right\rangle_k (t) - jk\omega_s \langle x \rangle_k (t). \tag{2}$$

It is important to point out that (2) corresponds to the exact derivative of the k^{th} coefficient only in the case that ω_s is constant. When the frequency is not constant, (2) is only a good approximation if ω_s is a slowly varying variable [2].

The generalized averaging method is applied to the series-parallel resonant converter shown on **Fig. 2**. Using the notation given in the figure and choosing $C_{o1'} = C_{o2'} = C_{o'}$, the differential equations that describe the circuit can be written as:

$$L_s \frac{di_{Ls}(t)}{dt} = -v_{Cs}(t) - v_{Cp}(t) + v_{AB}(t) \tag{3}$$

$$C_s \frac{dv_{Cs}(t)}{dt} = i_{Ls}(t) \tag{4}$$

$$C_{o'} \frac{dv_{o'}(t)}{dt} = abs(i_T) - \frac{2 \cdot v_{o'}(t)}{R_{o'}} \tag{5}$$

The state vector is given by $x(t) = \left[i_{Ls}(t) \;\; v_{Cs}(t) \;\; v_{o'}(t) \right]^T$. At this point, it is important to notice why the voltage in the parallel capacitor v_{cp} is not used as a state variable even though C_p is an energy storing element. In fact the v_{cp} waveform is not differentiable and its dynamic behavior is completely defined by the energy stored in L_s and in both output capacitors [3].

Fig. 3 shows the main waveforms of the simplified circuit of **Fig. 2** for a typical operating point. These waveforms are predominantly sinusoidal so it is assumed that the resonant current i_{Ls} and the voltage in the series capacitor v_{Cs} are well approximated by their first time-varying harmonic i.e. with the fundamental term of the Fourier series. The output voltage $v_{o'}$ is a DC voltage with slow dynamical behavior so it is assumed that it can be approximated with sufficient accuracy with the DC coefficient of the complex Fourier series. The nonlinear model for the dynamics of the local harmonics, assuming that the switching frequency varies slowly from one switching period to the next, is given by

$$\frac{d\langle I_{Ls} \rangle_1}{dt} = -j\omega_s \langle I_{Ls} \rangle_1 + \frac{1}{L_s}\left\{ -\langle V_{Cs} \rangle_1 - \langle V_{Cp} \rangle_1 + \langle V_{AB} \rangle_1 \right\} \tag{6}$$

$$\frac{d\langle V_{Cs} \rangle_1}{dt} = -j\omega_s \langle V_{Cs} \rangle_1 + \frac{1}{C_s}\langle I_{Ls} \rangle_1 \tag{7}$$

$$\frac{d\langle V_{o'} \rangle_0}{dt} = \frac{1}{C_{o'}}\left\{ abs(i_T)_1 - \frac{2 \cdot \langle V_{o'} \rangle_0}{R_{o'}} \right\} \tag{8}$$

where

$$\langle V_{AB} \rangle_1 = \frac{V_{in}}{\pi}\left[\sin(D\pi) + j(\cos(D\pi) - 1) \right] \tag{9}$$

$$\theta = \cos^{-1}\left(\frac{\omega_s C_p \langle V_{o'}\rangle_0}{2\cdot\left|\langle I_{Ls}\rangle_1\right|} - 1\right) \tag{10}$$

$$abs(i_T)_1 = \frac{2\cdot\left|\langle I_{Ls}\rangle_1\right|}{\pi}\cdot\left[1-\cos(\theta)\right] \tag{11}$$

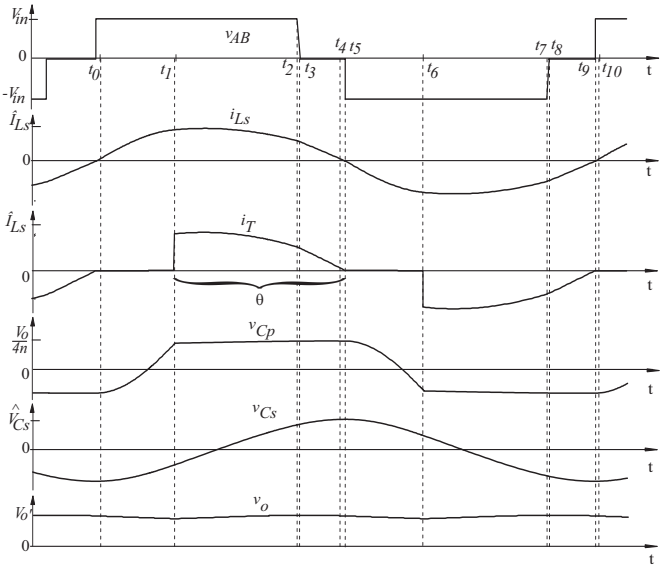

Fig. 3: Time behavior of the characteristic voltages and currents of a series-parallel resonant converter within a pulse period (t_0–t_{10}).

The new state variables are: $\langle I_{Ls}\rangle_1$, $\langle V_{Cs}\rangle_1$ and $\langle V_{o'}\rangle_0$. They are complex Fourier coefficients that can be written as a fifth order state space model with real variables: $\langle I_{Ls}\rangle_1 = x_1 + jx_2$, $\langle V_{Cs}\rangle_1 = x_3 + jx_4$ and $\langle V_{o'}\rangle_0 = x_7$. The voltage on the parallel capacitor can be also written as a function of real variables: $\langle V_{Cp}\rangle_1 = x_5 + jx_6$ [3].

Eq. (10) and (11) can be rewritten as:

$$\theta = \cos^{-1}\left(\frac{\omega_s C_p x_7}{2\cdot\sqrt{x_1^2+x_2^2}} - 1\right) \tag{12}$$

$$abs(i_T)_1 = \frac{2\cdot\sqrt{x_1^2+x_2^2}}{\pi}\cdot\left[1-\cos(\theta)\right] \tag{13}$$

As already stated, the voltage on the parallel capacitor is not considered as a state variable, so one needs to express this voltage as a function of the state variables. x_5 and x_6 are expressed as a function of the existing state variables x_1 and x_2.

$$x_5 = \frac{1}{\pi\omega_s C_p}\left[x_1\delta + x_2\gamma\right] \tag{14}$$

$$x_6 = \frac{1}{\pi\omega_s C_p}\left[x_2\delta - x_1\gamma\right] \tag{15}$$

where

$$\gamma = \pi - \theta + \frac{1}{2}\sin(2\theta) \tag{16}$$

$$\delta = \sin^2(\theta) \tag{17}$$

The new state vector is given by $x = \begin{bmatrix} x_1 & x_2 & x_3 & x_4 & x_7 \end{bmatrix}^T$ and the model with real variables is

$$\frac{dx_1}{dt} = \omega_s x_2 - \frac{x_3}{L_s} - \frac{x_5}{L_s} + \frac{V_{in}}{\pi\cdot L_s}\sin(D\pi) \tag{18}$$

$$\frac{dx_2}{dt} = -\omega_s x_1 - \frac{x_4}{L_s} - \frac{x_6}{L_s} + \frac{V_{in}}{\pi\cdot L_s}\left[\cos(D\pi) - 1\right] \tag{19}$$

$$\frac{dx_3}{dt} = \omega_s x_4 + \frac{x_1}{C_s} \tag{20}$$

$$\frac{dx_4}{dt} = -\omega_s x_3 + \frac{x_2}{C_s} \tag{21}$$

$$\frac{dx_7}{dt} = \frac{2\cdot\sqrt{x_1^2+x_2^2}}{\pi\cdot C_{o'}}\cdot\left[1-\cos(\theta)\right] - \frac{2\cdot x_7}{R_{o'}\cdot C_{o'}} \tag{22}$$

The switching frequency ω_s and duty cycle D are defined as the control inputs u_1 and u_2, respectively. The output voltage, the amplitude of the resonant current and the amplitude of the voltage in the series-capacitor are defined as the outputs y_1, y_2 and y_3, respectively.

$$u_1 = \omega_s \tag{23}$$

$$u_2 = D \tag{24}$$

$$y_1 = x_7 \tag{25}$$

$$y_2 = 2\cdot\sqrt{x_1^2+x_2^2} \tag{26}$$

$$y_3 = 2\cdot\sqrt{x_3^2+x_4^2} \tag{27}$$

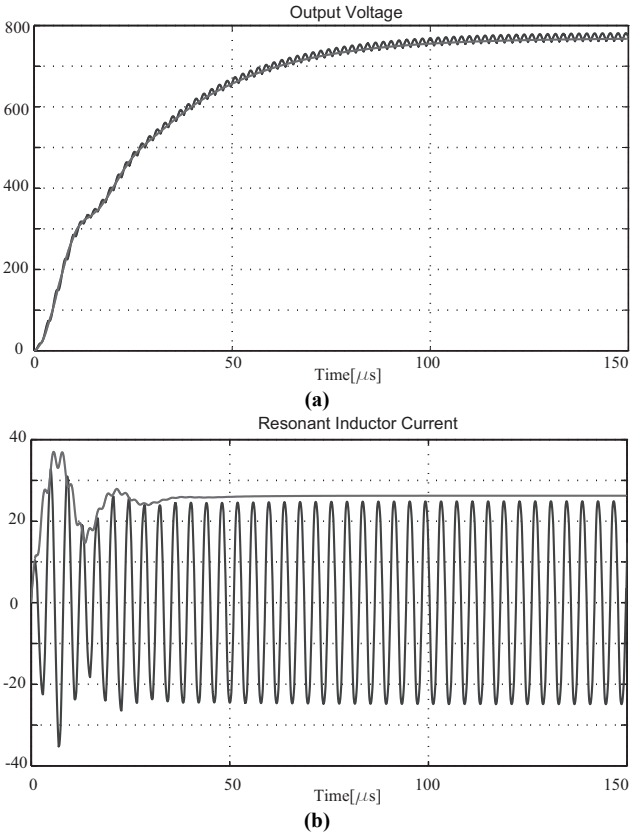

Fig. 4: Comparison of the amplitude of the model variables with the simulated waveforms: (a) output voltage $V_{o'}$ (100V/div); (b) resonant current i_{Ls} (10A/div).

Based on the generalized averaging model, digital simulations using MATLAB/SIMULINK are performed. The parameters used for the simulation are: $V_{o'} = 767$V, $P_o = 4.6$kW, $D = 0.752$, $f_s = 253$kHz and $R_{o'} = 128\Omega$. The simulation compares the magnitude of the complex coefficients obtained with the averaging method with the amplitude of the waveforms obtained simulating the switching circuit. The results for the resonant current and the equivalent output voltage referred to the primary side of the transformer are shown in **Fig. 4**. The results show that the correspondence between the waveforms obtained with the model and with the simulated circuit is excellent. Therefore the large signal model based on generalized averaging method is a good starting point to derive the small-signal model of the converter.

B. Small- Signal Model of the Series-Parallel Resonant Converter

In order to find the small-signal model for the series-parallel resonant converter with capacitive output filter the first step is to obtain a steady state solution for the system. This can be done setting the derivatives of Eq. (18)-(22) equal to zero. Furthermore the steady-state value of the angle θ is taken from [1]. The equations that represent the steady-state solution are given by

$$\theta_{ss} = 2 \cdot \tan^{-1} \sqrt{\frac{2\pi}{\omega_s C_p R_{o'}}} \tag{28}$$

$$\gamma_{ss} = \pi - \theta_{ss} + \frac{1}{2}\sin(2\theta_{ss}) \tag{29}$$

$$\delta_{ss} = \sin^2(\theta_{ss}) \tag{30}$$

$$\alpha = \frac{C_p}{C_s} \tag{31}$$

$$K = \frac{\omega_{s_{ss}} \cdot C_p \cdot V_{in}}{\delta_{ss}} \tag{32}$$

$$M = \frac{\delta_{ss}}{\gamma_{ss} + \pi \cdot \alpha - \pi \cdot \omega_{s_{ss}}{}^2 \cdot L_s \cdot C_p} \tag{33}$$

$$x_{1_{ss}} = -\frac{x_{2_{ss}}}{M} + K \cdot \sin(D\pi) \tag{34}$$

$$x_{2_{ss}} = \frac{K \cdot M^2}{(1+M^2)}\left\{\frac{\sin(D\pi)}{M} + \left[\cos(D\pi) - 1\right]\right\} \tag{35}$$

$$x_{3_{ss}} = \frac{x_{2_{ss}}}{\omega_{s_{ss}} \cdot C_s} \tag{36}$$

$$x_{4_{ss}} = -\frac{x_{1_{ss}}}{\omega_{s_{ss}} \cdot C_s} \tag{37}$$

$$x_{5_{ss}} = \frac{1}{\pi\omega_{s_{ss}} C_p}\left[x_{1_{ss}}\delta_{ss} + x_{2_{ss}}\gamma_{ss}\right] \tag{38}$$

$$x_{6_{ss}} = \frac{1}{\pi\omega_{s_{ss}} C_p}\left[x_{2_{ss}}\delta_{ss} - x_{1_{ss}}\gamma_{ss}\right] \tag{39}$$

$$x_{7_{ss}} = \frac{R_{o'}\sqrt{x_{1_{ss}}{}^2 + x_{2_{ss}}{}^2}}{\pi}\left[1 - \cos(\theta_{ss})\right] \tag{40}$$

After obtaining the steady-state solution, the model can be linearized around the steady state in order to obtain the small-signal transfer functions from any desired input to any desired output. After the linearization one obtains a linearized model of the type given by Eq. (41).

$$\begin{cases} \dot{\vec{\Delta x}} = A\vec{\Delta x} + B\vec{\Delta u} \\ \vec{\Delta y} = C\vec{\Delta x} + D\vec{\Delta u} \end{cases} \tag{41}$$

where A, B, C and D are matrices that describe the system, $\vec{x}$ is the state vector, $\vec{u}$ is the input vector, $\vec{y}$ is the output vector and Δ means the small changes of the respective parameter.

It is important to point out that steady state solution is dependent on the operating point of the system (desired output voltage and load). Thus, there is one steady state solution for each operating point of the system. This makes the analytical linearization of the system complex. The complete set of equations is presented in the Appendix of this paper. However, if one is interested in a specific operation point then the numerical solutions are easily computed with software such as MATLAB. Therefore this procedure can be used to calculate transfer functions for desired operating points in a fast and reliable way.

With the linear system formed by the matrices A, B, C, D one is in position to obtain the six transfer functions that relate the control input u_1 (switching frequency) or u_2 (duty cycle, D) to the outputs y_1 (output voltage), y_2 (amplitude of the resonant current) or y_3, (amplitude of the voltage in the series capacitor). The transfer functions that relate the inputs u_1, u_2 with the output y_1, are particularly interesting because the main control purpose is to adjust the output voltage to any desired reference value for all kind of load changes. The switching frequency of the converter is automatically adjusted to ensure zero-current switching of one bridge leg where the output power is controlled by duty cycle variation. Therefore, the transfer function that is essential for the controller design is the transfer function that relates duty cycle with output voltage $G(s) = \Delta V_{o'} / \Delta D = \Delta y_1 / \Delta u_2$.

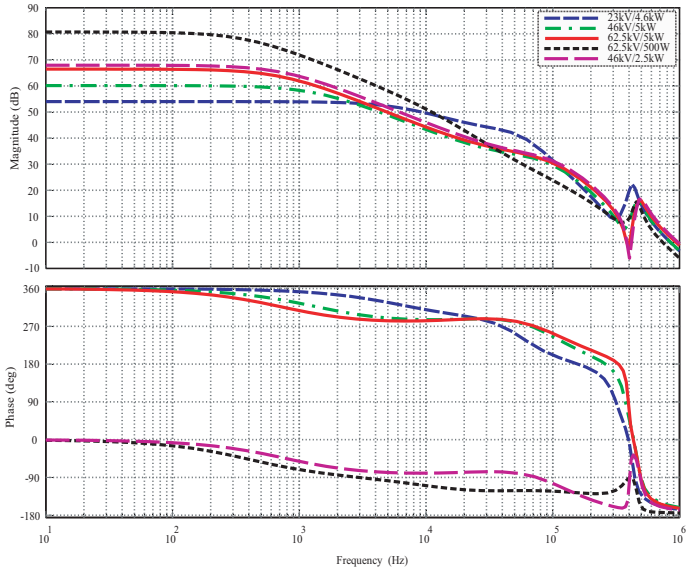

Fig. 5: Bode plots of $G(s)$ for different operating points of the system.

IV. SIMULATION RESULTS

Fig. 5 presented the Bode magnitude and phase plots of the output voltage for small changes in duty cycle. They represent the transfer function $G(s)$ for different load conditions from full power to very low power. The five different output voltage / output power operating points are: 23kV/4.6kW, 46kV/5kW, 62.5kV/5kW, 62.5kV/0.5kW and 46kV/2.5kW. These points are arbitrarily

chosen just in order to show how the transfer function changes within the operating range of the converter.

One can see that the DC gain of the transfer function *G(s)* changes significantly with the load. The phase plot shows that for some load conditions the transfer function has two non minimum phase zeros, which indicates that the system is difficult to control. This characteristic is evident comparing phase transitions for the same output voltage, 62.5kV, and different output power, 5kW and 500W. For 5kW the system is non minimum phase and for 500W is minimum phase. Thus a very robust control technique is needed in order to overcome this difficulty. The peaks in the magnitude correspond to summation of the series resonant frequency f_o and the switching frequency f_s.

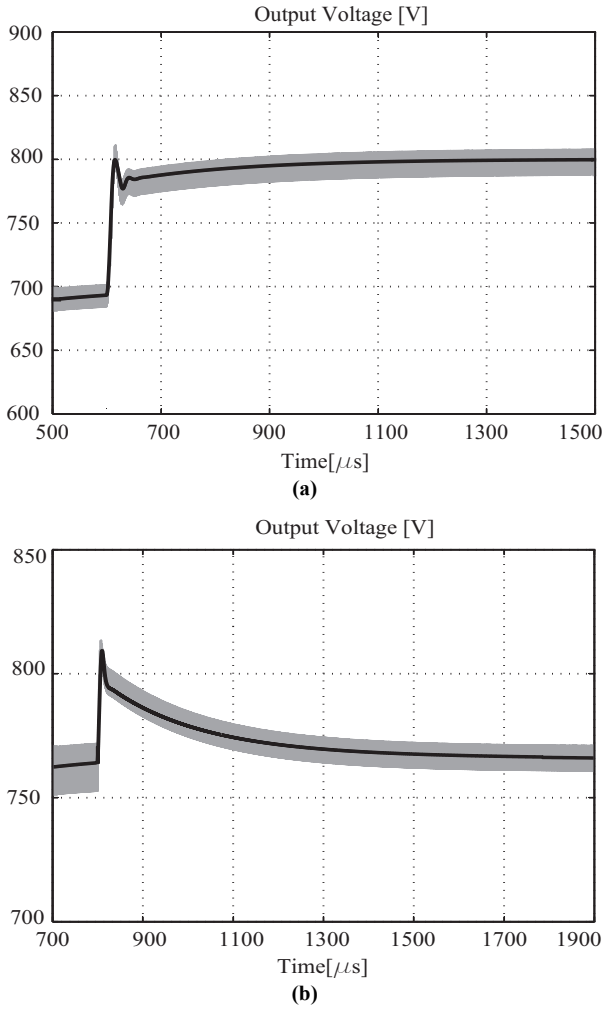

Fig. 6: Comparison between step response of the linearized model and of the circuit (a) with a step change in the value of reference voltage and (b) with a step change in the value of the load resistance. Scale: output voltage V_o. (50V/div).

In order to prove that the small-signal model well approximates the converter, simulations using MATLAB were undertaken for various load and reference output voltage steps. **Fig. 6(a)** shows a comparison between the simulated switching circuit with a constant load and the linearized model. It represents the closed loop response to a step change in the reference voltage $V_{o'ref}$ from 700V to 800V using a PI controller with fixed parameters. **Fig. 6(b)** shows a comparison between the simulated switching circuit and the linearized model when a load change occurs. This represents the step response when the reference voltage (referred to the primary side of the transformer) is held constant at 767V and the output power is reduced from 4.6kW to 2.3kW.

From the results shown in **Fig. 6**, one can conclude that the linearized model agrees well with the dynamics of the simulated converter. Therefore the calculation method is valid and is a very helpful tool for the control design.

V. EXPERIMENTAL RESULTS

In order to verify if the results obtained theoretically and with digital simulations are reproducible in practice, a 5kW prototype is built. Since the objective of the laboratory tests is only to verify the validity of the small-signal representation, one does not have to construct the complete high-voltage converter. It is sufficient to build the equivalent circuit shown in **Fig. 2** with all quantities referred to the primary side of the transformer. Thus, the prototype is constructed without high-voltage transformer. The parasitic elements (leakage inductance and stray capacitance), which are necessary to build the resonant circuit, are replaced with external elements. The photograph of the constructed prototype of the equivalent system is shown in **Fig. 7.**

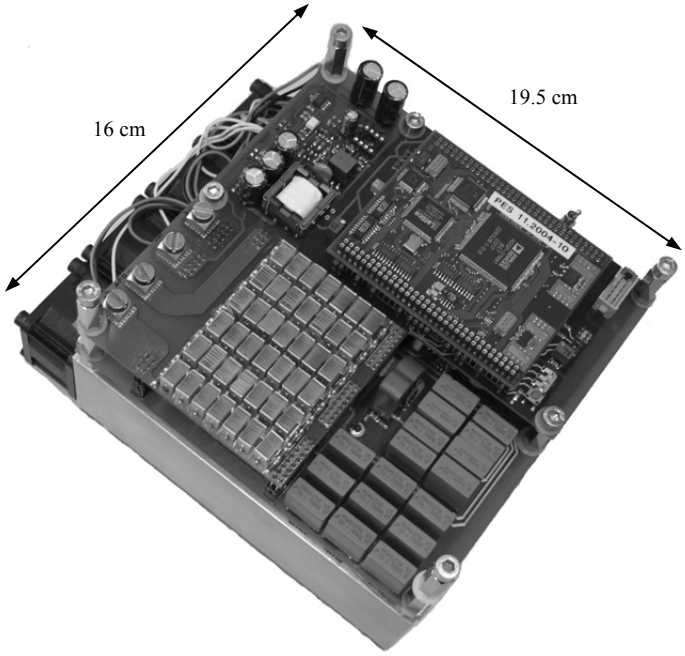

Fig. 7: Photograph of the 5kW prototype of the series-parallel resonant converter with capacitive output filter.

Fig. 8 shows the comparison between the results obtained with simulation and from the laboratory tests without the high-voltage transformer. This represents the closed loop response of the system when a step change in the reference voltage occurs. At time of 0.1ms the reference voltage is changed from 410V to 750V. In the figure, one can see that the rise time, which is about 100μs, is the same for both simulated and experimental waveforms. The small differences between both waveforms are due to approximations used in the development of the model and to the unmodeled non-idealities of the real circuit. In the practical implementation the reference voltage passes through a first order proportional/lag element before it is compared with the measured voltage.

Therefore the measured output voltage is compared with a reference voltage that has an exponential rise rather than a step change. Since the controller is very fast, the controller sets the duty cycle immediately to the maximum value when a step occurs and the output voltage is, for a short time, higher than the reference voltage. The controller then reduces the duty cycle to a minimum value and this transient behavior is responsible for the plateau that occurs from time 0.2ms to 0.3ms in the experimental waveform before the output voltage reaches its final value. Even considering this small difference between both waveforms, there is a good agreement between the simulation results using the proposed small-signal model and the experimental result.

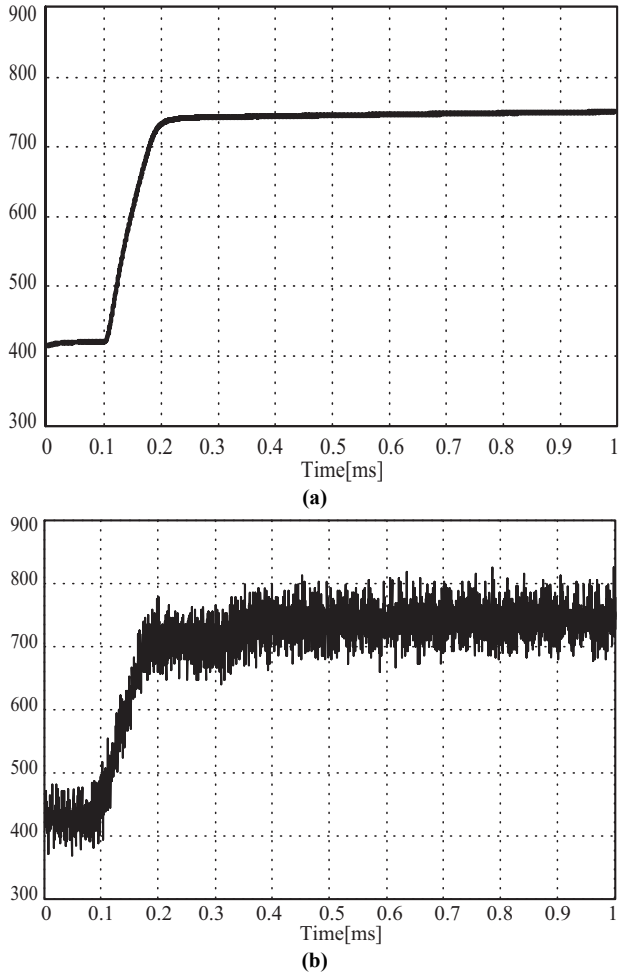

Fig. 8: Closed-loop response of the output voltage for a step change in the reference from 410V to 750V: (a) Simulation result using the proposed model (b) Experimental result. Scale: output voltage V_o (100V/div), Time (100μs/div).

VI. CONCLUSIONS

This paper presents an accurate method, based on first harmonic analysis, to derive the small-signal model of the series-parallel resonant DC-DC converter with capacitive output filter. The model provides a fast and reliable way to obtain desired transfer functions of the system for each operating point. For this reason, the small-signal model simplifies the controller design task for resonant converters by removing the need of complex mathematical analysis and saves the time required for measurements in the trial and error design method.

APPENDIX

Matrix A is a 5x5 system matrix and it gives the relation between the derivative of states and the states.

$$A=\begin{bmatrix} a_{11} & a_{12} & a_{13} & 0 & a_{15} \\ a_{21} & a_{22} & 0 & a_{24} & a_{25} \\ a_{31} & 0 & 0 & a_{34} & 0 \\ 0 & a_{42} & a_{43} & 0 & 0 \\ a_{51} & a_{52} & 0 & 0 & a_{55} \end{bmatrix}$$

where

$$I_{1_{ss}}=\sqrt{{x_{1_{ss}}}^2+{x_{2_{ss}}}^2} \tag{A.1}$$

$$G_1=\frac{{x_{7_{ss}}}^2\cdot\omega_s\cdot C_p}{4\cdot\pi\cdot L_s\cdot{I_{1_{ss}}}^2}-\frac{x_{7_{ss}}}{\pi\cdot L_s\cdot I_{1_{ss}}} \tag{A.2}$$

$$G_2=\left(\frac{x_{7_{ss}}}{\pi\cdot L_s\cdot I_{1_{ss}}}-\frac{{x_{7_{ss}}}^2\cdot\omega_s\cdot C_p}{2\cdot\pi\cdot L_s\cdot{I_{1_{ss}}}^2}\right) \tag{A.3}$$

$$G_3=\frac{2}{\pi\cdot\omega_s\cdot C_p\cdot L_s\cdot{I_{1_{ss}}}^2\cdot\tan\left(\frac{\theta_{ss}}{2}\right)}+\frac{{x_{7_{ss}}}^2\cdot\omega_s\cdot C_p\cdot\tan\left(\frac{\theta_{ss}}{2}\right)}{2\cdot\pi\cdot L_s\cdot{I_{1_{ss}}}^4} -\frac{x_{7_{ss}}}{2\cdot\pi\cdot L_s\cdot{I_{1_{ss}}}^3}\left(\tan\left(\frac{\theta_{ss}}{2}\right)+\frac{1}{\tan\left(\frac{\theta_{ss}}{2}\right)}\right) \tag{A.4}$$

$$G_4=\omega_s-\frac{1}{\omega_s\cdot C_p\cdot L_s}+\frac{\theta_{ss}}{\pi\cdot\omega_s\cdot C_p\cdot L_s} \tag{A.5}$$

$$a_{11}=G_1+\frac{{x_{1_{ss}}}^2}{{I_{1_{ss}}}^2}\cdot G_2+x_{1_{ss}}\cdot x_{2_{ss}}\cdot G_3 \tag{A.6}$$

$$a_{12}=\left[\frac{x_{1_{ss}}\cdot x_{2_{ss}}}{{I_{1_{ss}}}^2}+\frac{1}{2}\tan\left(\frac{\theta_{ss}}{2}\right)\right]\cdot G_2+{x_{2_{ss}}}^2\cdot G_3+G_4 \tag{A.7}$$

$$a_{13}=-\frac{1}{L_s} \tag{A.8}$$

$$a_{15}=-\frac{x_{1_{ss}}}{x_{7_{ss}}}\cdot G_2-\frac{x_{2_{ss}}\cdot{I_{1_{ss}}}^2}{x_{7_{ss}}}G_3 \tag{A.9}$$

$$a_{21}=\left[\frac{x_{1_{ss}}\cdot x_{2_{ss}}}{{I_{1_{ss}}}^2}-\frac{1}{2}\tan\left(\frac{\theta_{ss}}{2}\right)\right]\cdot G_2-{x_{1_{ss}}}^2\cdot G_3-G_4 \tag{A.10}$$

$$a_{22}=G_1+{x_{2_{ss}}}^2\cdot G_2-x_{1_{ss}}\cdot x_{2_{ss}}\cdot G_3 \tag{A.11}$$

$$a_{24}=-\frac{1}{L_s} \tag{A.12}$$

$$a_{25}=-\frac{x_{2_{ss}}}{x_{7_{ss}}}\cdot G_2+\frac{x_{1_{ss}}\cdot{I_{1_{ss}}}^2}{x_{7_{ss}}}G_3 \tag{A.13}$$

$$a_{31}=\frac{1}{C_s} \tag{A.14}$$

$$a_{34}=\omega_s \tag{A.15}$$

$$a_{42}=\frac{1}{C_s} \tag{A.16}$$

$$a_{43} = -\omega_s \tag{A.17}$$

$$a_{51} = \frac{4 \cdot x_{1_{ss}}}{\pi \cdot C_{o'} \cdot I_{1_{ss}}} \tag{A.18}$$

$$a_{52} = \frac{4 \cdot x_{2_{ss}}}{\pi \cdot C_{o'} \cdot I_{1_{ss}}} \tag{A.19}$$

$$a_{55} = -\frac{1}{C_{o'}}\left(\frac{\omega_s \cdot C_p}{\pi} + \frac{2}{R_{o'}}\right) \tag{A.20}$$

B is the input matrix and it relates the derivative of the states with the system inputs. The two inputs, *D* and ω_s are used resulting in a 5x2 matrix for *B*.

$$B = \begin{bmatrix} b_{11} & b_{12} \\ b_{21} & b_{22} \\ b_{31} & 0 \\ b_{41} & 0 \\ b_{51} & 0 \end{bmatrix}$$

where

$$H_1 = \frac{x_{7_{ss}}{}^2 \cdot C_p}{4 \cdot \pi \cdot L_s \cdot I_{1_{ss}}{}^2} \tag{A.21}$$

$$H_2 = 1 + \frac{1}{\omega_s^2 \cdot C_p \cdot L_s} - \frac{\theta_{ss}}{\pi \cdot \omega_s^2 \cdot C_p \cdot L_s} - \frac{2}{\pi \cdot \omega_s^2 \cdot C_p \cdot L_s \cdot \tan\left(\frac{\theta_{ss}}{2}\right)}$$

$$- \frac{x_{7_{ss}}{}^2 \cdot C_p \cdot \tan\left(\frac{\theta_{ss}}{2}\right)}{4 \cdot \pi \cdot L_s \cdot I_{1_{ss}}{}^2} + \frac{x_{7_{ss}}}{2 \cdot \pi \cdot \omega_s \cdot L_s \cdot I_{1_{ss}} \cdot \tan\left(\frac{\theta_{ss}}{2}\right)} \tag{A.22}$$

$$b_{11} = x_{1_{ss}} \cdot H_1 + x_{2_{ss}} \cdot H_2 \tag{A.23}$$

$$b_{21} = x_{2_{ss}} \cdot H_1 - x_{1_{ss}} \cdot H_2 \tag{A.24}$$

$$b_{31} = x_{4_{ss}} \tag{A.25}$$

$$b_{41} = -x_{3_{ss}} \tag{A.26}$$

$$b_{51} = -\frac{x_{7_{ss}} \cdot C_p}{\pi \cdot C_{o'}} \tag{A.27}$$

$$b_{12} = \frac{V_{in}}{L_s}\cos(D\pi) \tag{A.28}$$

$$b_{22} = -\frac{V_{in}}{L_s}\sin(D\pi) \tag{A.29}$$

The matrix that relates the states with the output is the *C* matrix. There are three outputs and five states thus *C* is a 3x5 matrix.

$$C = \begin{bmatrix} 0 & 0 & 0 & 0 & 1 \\ c_{21} & c_{22} & 0 & 0 & 0 \\ 0 & 0 & c_{33} & c_{34} & 0 \end{bmatrix}$$

where

$$V_{1_{ss}} = \sqrt{x_{3_{ss}}{}^2 + x_{4_{ss}}{}^2} \tag{A.30}$$

$$c_{21} = \frac{2 \cdot x_{1_{ss}}}{I_{1_{ss}}} \tag{A.31}$$

$$c_{22} = \frac{2 \cdot x_{2_{ss}}}{I_{1_{ss}}} \tag{A.32}$$

$$c_{33} = \frac{2 \cdot x_{3_{ss}}}{V_{1_{ss}}} \tag{A.33}$$

$$c_{34} = \frac{2 \cdot x_{4_{ss}}}{V_{1_{ss}}} \tag{A.34}$$

Finally, matrix *D* is called the direct transmission matrix and it represents the elements that transmit an input directly to the output of the system. For our case *D* is a 3x2 zero matrix.

REFERENCES

[1] F.S. Cavalcante and J.W. Kolar, "Design of a 5kW High Output Voltage Series-Parallel Resonant DC-DC Converter," in *Proceedings of the 34th IEEE Power Electronics Specialists Conference*, Acapulco, Mexico, 2003, vol. 4, pp. 1807 - 1814.

[2] S.R. Sanders, J.M. Noworolski, X.Z. Liu, et al. "Generalized Averaging Method for Power Conversion Circuits," *IEEE Transactions on Power Electronics*, vol. 6, no. 2, pp. 251-259, April 1991.

[3] J.A. Martín-Ramos, J. Diaz, A.M. Pernía, et al. "Large-Signal Modeling of the PRC-LCC Resonant Topology with a Capacitor as Output Filter," in *Proceedings of the 17th Annual IEEE Applied Power Electronics Conference and Exposition*, Dallas, TX, 2002, vol. 2, pp. 1120 - 1126.

[4] V. Vorpérian, "Approximate Small-Signal Analysis of the Series and the Parallel Resonant Converters," *IEEE Transactions on Power Electronics*, vol. 4, no. 1, pp. 15-24, January 1989.

[5] E.X. Yang, B. Choi, F.C. Lee, et al. "Dynamic Analysis and Control Design of LCC Resonant Converter," in *Proceedings of the 23rd Power Electronics Specialists Conference*, Toledo, Spain, 1992, vol. 1, pp. 362 – 369.

[6] A.M. Stankovic, D.J. Perreault, K. Sato, et al. "Analysis and Experimentation with Dissipative Nonlinear Controllers for Series Resonant DC/DC Converters," in *Proceedings of the 28th Power Electronics Specialists Conference*, St. Louis, MI, 1997, vol. 1, pp. 679 – 685.

[7] G. Garcia Soto, J. Gaysse, G.W. Baptiste, "Variable Sampling Time Serial-Resonant Current Converter Control for a High-Voltage X-ray Tube Application," in *Proceedings of the 10th European Power Quality Conference*, Nuremberg, Germany, 2004, pp. 972 - 977.